



Role of Multiple Calcium and Calcium-Dependent Conductances in Regulation of Hippocampal Dentate Granule Cell Excitability

ILDIKÓ ARADI AND WILLIAM R. HOLMES

Neuroscience Program, Department of Biological Sciences, Ohio University, Athens, OH 45701

aradi@ohiou.edu

holmes@ohiou.edu

Received April 2, 1998; Revised August 25, 1998; Accepted September 22, 1998

Action Editor: Steve Redman

Abstract. We have constructed a detailed model of a hippocampal dentate granule (DG) cell that includes nine different channel types. Channel densities and distributions were chosen to reproduce reported physiological responses observed in normal solution and when blockers were applied. The model was used to explore the contribution of each channel type to spiking behavior with particular emphasis on the mechanisms underlying postspike events. T-type calcium current in more distal dendrites contributed prominently to the appearance of the depolarizing after-potential, and its effect was controlled by activation of BK-type calcium-dependent potassium channels. Co-activation and interaction of N-, and/or L-type calcium and AHP currents present in somatic and proximal dendritic regions contributed to the adaptive properties of the model DG cell in response to long-lasting current injection. The model was used to predict changes in channel densities that could lead to epileptogenic burst discharges and to predict the effect of altered buffering capacity on firing behavior. We conclude that the clustered spatial distributions of calcium related channels, the presence of slow delayed rectifier potassium currents in dendrites, and calcium buffering properties, together, might explain the resistance of DG cells to the development of epileptogenic burst discharges.

Keywords: hippocampus, dentate, calcium channels, potassium channels, afterpotentials, AHP, DAP, burst, calcium-dependent potassium channels, compartmental model

Introduction

The dentate granule (DG) cell, one of the principal cells of the dentate gyrus, receives synaptic input from the perforant path of the entorhinal cortex and sends its major projection toward pyramidal cells in hippocampal CA3 region. It is known that DG cells are resistant to the development of epileptogenic burst discharges following disinhibition in contrast to neocortical and hippocampal pyramidal neurons (Fricke and Prince, 1984). This nonbursting behavior may be related either to the absence of significant recurrent excitatory circuitry within the dentate gyrus itself or to the DG cell's intrinsic voltage dependent ionic currents.

Firing properties of DG cells have been well studied. These cells have a characteristic firing threshold, latency to firing, and action potential width. Under physiological conditions, a short current stimulus or brief synaptic activation can evoke up to three consecutive spikes (Fricke and Prince, 1984). Spikes evoked either by antidromic or orthodromic stimulation are always followed by a depolarizing after-potential (DAP) and a long-lasting after-hyperpolarization (AHP) (Crunelli et al., 1983; Zhang et al., 1993). The DAP occurs in an all-or-none fashion along with the generation of the action potentials (AP). However, graded DAP-like responses also can be evoked by suprathreshold depolarizing pulses or by stimulation in the presence

of tetrodotoxin (TTX) (Zhang et al., 1993). Repetitive firing evoked by long current pulses shows spike frequency adaptation presumably due to the activation of calcium-dependent potassium conductances.

DG cells are known to express at least three distinct types of voltage-gated calcium and two types of calcium activated potassium channels (Blaxter et al., 1989; Fisher et al., 1990; Eliot and Johnston, 1994; Beck et al., 1997). Although calcium conductances have been suggested to contribute to the DAP (Zhang et al., 1993), the actual mechanism has not been determined. On the basis of pharmacological and other properties, T-type channels have been suggested to underlie the DAP in DG cells (Zhang et al., 1993). However, this large postspike depolarizing component looks very similar to the calcium spike observed by Blaxter et al. (1989) and Fricke and Prince (1984), which was proposed to be generated mainly by activation of an N-type calcium current (Blaxter et al., 1989). It is important to ask which voltage gated calcium-channel(s) supplies the calcium to activate particular calcium-dependent potassium conductances because these interacting conductances cause postspike potentials, such as the DAP and AHP, which play a significant role in regulating neuronal excitability. An anatomical, functional colocalization and thus coactivation of calcium-related channels has been shown (Roberts et al., 1990; Robitaille et al., 1993), but there is a need for further studies.

Yuen and Durand (1991) developed a model of a hippocampal granule cell with four different ionic conductances. Several electrophysiological characteristics of DG cells could be reproduced by this model, but it failed to reproduce correctly after-spike events, particularly the shape and size of the DAP. Because one of the most characteristic features of the DG cell's spiking behavior is that APs are always followed by a large DAP, we have created and investigated models that included detailed morphology and nine voltage- and/or calcium-dependent ionic channels. We explored the possible contribution of calcium-related channels to the generation and modulation of postspike events. Though very little is known about the spatial distribution of these channels, the model, through comparisons to published experimental data, allowed us to deduce likely clustered spatial distributions of distinct calcium-related channel types and their functional role in the excitability of DG cells and to explore possible reasons for the resistance of DG cells to the development of epileptogenic burst discharges.

Methods

Model Morphology and Passive Parameters

Models of DG cells were created where morphological details were taken into account at different levels of precision. A reduced model of a DG cell was used for preliminary studies to investigate the possible mechanisms underlying the DAP and coactivation of calcium-related channels and to give estimates for the values of channel densities. A model with a fully reconstructed dendritic tree was used to reproduce the characteristic responses of DG cells to current injections and to study the effects of channel blockers. In both cases dendritic spines were implicitly taken into account by reducing membrane resistivity and increasing membrane capacity according to the portion of total membrane area due to spines (Rall et al., 1992) using spine densities from Desmond and Levy (1985).

Figure 1 shows the morphology of a real DG cell used in full morphology model simulations (Desmond and Levy, 1982, 1984) and the schematic picture of a reduced morphology model used in other simulations. Table 1 contains details of the number of compartments in the reduced model and passive parameters for both models. The input resistance of the model cells measured at the soma was 250 to 270 M Ω , and the membrane time constant was 40 ms consistent with values found experimentally (Staley et al., 1992; Spruston and Johnston, 1992).

Our simulations were performed with the GENESIS simulation program (Bower and Beeman, 1995) using the Hines algorithm (Hines, 1995) with a time step of 0.01 ms.

Modeled Voltage- and Calcium-Dependent Conductances

Six functionally different parts of DG cells were described with different densities of active channels. These were the axon, soma, granule cell layer dendrites (GCLD), and the proximal (PD), middle (MD), and distal (DD) thirds of the dendritic tree.

To simulate the basic active properties of DG cells, nine channel types were included in the model: fast sodium (Na), fast delayed rectifier potassium (fK_{DR}), slow delayed rectifier potassium (sK_{DR}), A-type potassium (K_A), large conductance calcium- and voltage-dependent potassium (BK), small conductance calcium-dependent potassium (SK) channels,

Table 1. The passive parameters of the model DG cell.

	R_m	R_A	C_m	n	l	l/n	d	L/n
Axon-1	40,000	210	1	1	50	50	0.9	0.0762
Axon-2	40,000	210	1	1	50	50	0.7	0.0866
Axon-3	40,000	210	1	1	50	50	0.5	0.102
Axon-4	40,000	210	1	28	1400	50	0.4	0.11465
Soma	40,000	210	1	2	16.8	8.4	16.8	0.00105
GCLD	40,000	210	1	2	50	25	3	0.0209
PD	25,000	210	1.6	4	150	37.5	3	0.042
MD	25,000	210	1.6	4	150	37.5	3	0.042
DD	25,000	210	1.6	4	150	37.5	3	0.042

Note: GCLD, granule cell layer dendrites; PD, proximal dendrites; MD, middle dendrites; DD, distal dendrites; R_m (Ωcm^2), membrane resistivity; R_A (Ωcm), axial resistivity; C_m ($\mu\text{F}/\text{cm}^2$), specific membrane capacitance; n , the number of compartments in the reduced model; l (μm), the length of a region; d (μm), the diameter of a compartment; L , the electrotonic length of a region; and L/n , the electrotonic length of a compartment.

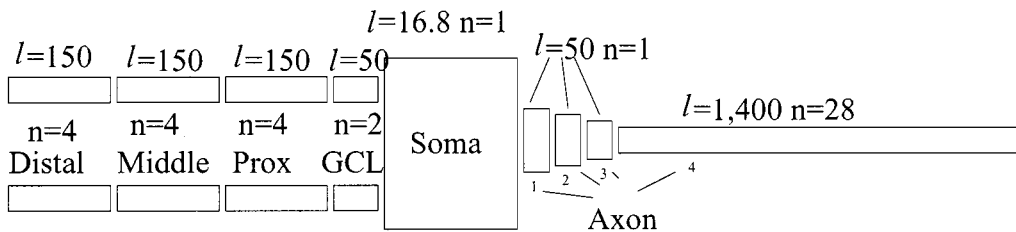
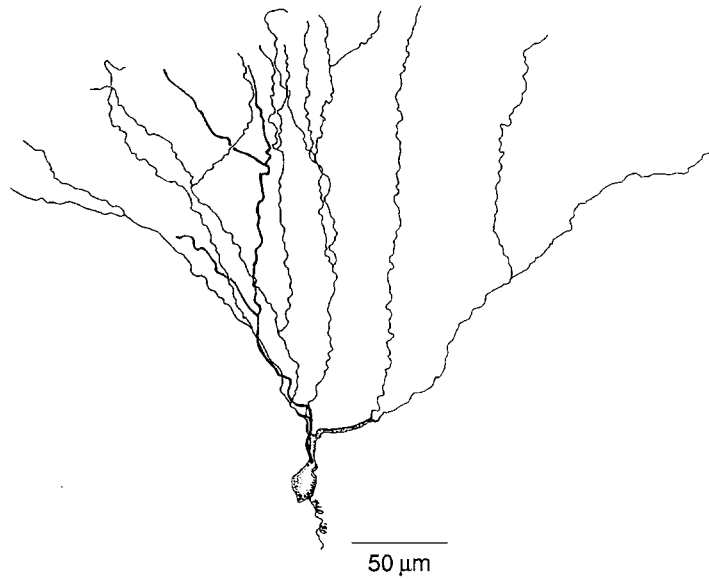


Figure 1. Cell used in the simulations and schematic picture of the structure of the reduced model DG cell. In the reduced and full morphology models we distinguished six regions of the DG cell having different distributions of voltage-activated channels—the soma, axon, granule cell layer dendrites, proximal, middle, and distal dendrites. In the lower figure l denotes the length in μm of a region where channels are distributed uniformly, and n is the number of compartments. Other passive parameter values used in the models are collected in Table 1.

and T-type (TCa), N-type (NCa), and L-type (LCa) calcium channels. These channel types were described by Hodgkin-Huxley-like equations, where channel kinetics were chosen as described below (with units of mV and ms for voltage and time).

Fast Sodium Current. Equations for the fast sodium channel were taken from Yuen and Durand (1991) except that the voltage dependence was shifted by 16 mV to obtain a proper threshold value for the generated action potential. The equations for I_{Na} current are

$$I_{Na} = G_{Na}(V, t) \cdot (V - E_{Na}), \quad E_{Na} = 45 \text{ mV}$$

$$G_{Na}(V, t) = g_{Na}^{\max} \cdot m^3(V, t) \cdot h(V, t)$$

$$\alpha_m(V) = -0.3(V - 25) / (e^{(V-25)/-5} - 1)$$

$$\beta_m(V) = 0.3(V - 53) / (e^{(V-53)/5} - 1)$$

$$\alpha_h(V) = 0.23 / e^{(V-3)/20}$$

$$\beta_h(V) = 3.33 / (e^{(V-55.5)/-10} + 1).$$

Fast and Slow Delayed Rectifier Potassium Currents.

The kinetic description for the fast delayed rectifier potassium current ($I_{fK_{DR}}$) was also taken from Yuen and Durand (1991) with the voltage dependence shifted by 16 mV.

The equations for $I_{fK_{DR}}$ current are

$$I_{fK_{DR}} = G_{fK_{DR}}(V, t) \cdot (V - E_K),$$

$$E_K = -85 \text{ mV}$$

$$G_{fK_{DR}}(V, t) = g_{fK_{DR}}^{\max} \cdot n_f^4(V, t)$$

$$\alpha_{n_f}(V) = -0.07(V - 47) / (e^{(V-47)/-6} - 1)$$

$$\beta_{n_f}(V) = 0.264 / e^{(V-22)/40}.$$

Though the term *delayed rectifier* has generally been applied to several different kinds of potassium currents, a large portion of the hippocampal potassium current seems to belong to a slow group of delayed rectifier currents (Storm, 1990; Beck et al., 1992). We introduced a slow delayed rectifier current to control the slower component of the repolarization processes in the DG cell dendrites. To describe this slow delayed rectifier current, we used the equations for $I_{fK_{DR}}$, but with activation chosen to be less than half as fast (that is, the τ_{fast} value was 40% of τ_{slow}). The activation curve of this current was shifted to more negative values by 12 mV compared to the fK_{DR} above. Consequently, the

equations for the $I_{sK_{DR}}$ became the following:

$$I_{sK_{DR}} = G_{sK_{DR}}(V, t) \cdot (V - E_K),$$

$$E_K = -85 \text{ mV}$$

$$G_{sK_{DR}}(V, t) = g_{sK_{DR}}^{\max} \cdot n_s^4(V, t)$$

$$\alpha_{n_s}(V) = -0.028(V - 35) / (e^{(V-35)/-6} - 1)$$

$$\beta_{n_s}(V) = 0.1056 / e^{(V-10)/40}.$$

A-Type Potassium Current. The presence of a 4-aminopyridine (4-AP) sensitive conductance in hippocampal granule cells was shown by Beck et al. (1992, 1997). The activation and inactivation characteristics were similar to those described for many other members of the A current family in different hippocampal preparations (Numann et al., 1987; Segal et al., 1984). This channel has been reported to delay (up to 100 ms) the onset of the action potential, raise excitation threshold, and modulate the initial part of action potential repolarization (Storm, 1990). Activation and inactivation gate parameters were based on those of Warman et al. (1994), which describe the A-type current reported by Numann et al. (1987) in guinea pig CA1 neurons. We shifted the activation and inactivation curves, 5 mV more negative and 5 mV more positive, respectively, to enhance this conductance near the resting potential of DG cell. Thus equations for A-type potassium current were

$$I_{K_A} = G_{K_A}(V, t) \cdot (V - E_K), \quad E_K = -85 \text{ mV}$$

$$G_{K_A}(V, t) = g_{K_A}^{\max} \cdot k(V, t) \cdot l(V, t)$$

$$\alpha_k(V) = -0.05(V + 25) / (e^{(V+25)/-15} - 1)$$

$$\beta_k(V) = 0.1(V + 15) / (e^{(V+15)/8} - 1)$$

$$\alpha_l(V) = 0.00015 / e^{(V+13)/15}$$

$$\beta_l(V) = 0.06 / (e^{(V+68)/-12} + 1).$$

Calcium Channels. At least three voltage-gated calcium channels, commonly referred to as T-, N-, and L-type channels with unitary conductances of 8, 14, and 25 pS have been described for dentate granule cells (Blaxter et al., 1989; Fisher et al., 1990).

The transient low threshold (TLT) calcium current in granule cells (Blaxter et al., 1989) resembles the T-type current described by Fox et al. (1987a, 1987b). Both of these currents were activated by small depolarizing test pulses from relatively hyperpolarized holding

potentials and inactivated by maintained depolarized holding potentials and were brief, lasting between 100 and 200 ms. Furthermore, Blaxter's data characterize this T-like current as relatively insensitive to repetitive activation. Several experiments showed that Ni^{2+} and Co^{2+} ions have a preferential blocking effect on T-type calcium current (Zhang et al., 1993; Eliot and Johnston, 1994).

The transient high threshold (THT) calcium-current in granule cells (Blaxter et al., 1989) has many features of the N current described by Fox et al. (1987a, 1987b), because it requires a prolonged negative holding potential for complete removal of inactivation and has an activation threshold that is more positive than the TLT. The THT current is supposed to be responsible for the large calcium spike. There are several lines of evidence to support this, as it is the largest of three calcium currents (see also Eliot and Johnston, 1994), and both the THT current in these experiments and calcium spikes in CA1 neurons rapidly diminished with repetitive action potentials.

Sustained high- and low-threshold (SHT and SLT, respectively) calcium currents were also described in hippocampal granule cells (Blaxter et al., 1989), which resemble the L-type current described by Fox et al. (1987a, 1987b), since both are activated from depolarized holding potentials and show little inactivation during prolonged depolarization. Blaxter's data make a further distinction between these sustained currents by their incremental decay to repetitive activation. The kinetics used for the T-, N-, and L-type calcium channels were taken from Jaffe et al. (1994).

The reversal potential for calcium, E_{Ca} , was calculated at each time step with the Nernst equation to accommodate changes in the driving force due to changes in intracellular calcium concentration. Calcium concentration was computed in a narrow shell just beneath the cell membrane for each compartment given inward calcium current and calcium removal. The rate of change of the intracellular calcium concentration was given by

$$\frac{d[\text{Ca}^{2+}](t)}{dt} = B \sum_{T,N,L} I_{\text{Ca}} - \frac{[\text{Ca}^{2+}](t) - [\text{Ca}^{2+}]_0}{\tau}$$

where $B = 5.2 \cdot 10^{-6}/Ad$ in units of $\text{mol}/(\text{C} \cdot \text{m}^3)$ for a shell of surface area A and thickness d ($0.2 \mu\text{m}$) and $\tau = 9$ ms was the calcium removal rate (Yuen and Durand, 1991). $[\text{Ca}^{2+}]_0 = 70$ nM was the resting calcium concentration.

The equations for calcium channels were

$$I_{\text{TCa}} = G_{\text{TCa}}(V, t) \cdot (V - E_{\text{Ca}})$$

$$G_{\text{TCa}}(V, t) = g_{\text{TCa}}^{\text{max}} \cdot a^2(V, t) \cdot b(V, t)$$

$$\alpha_a(V) = 0.2(19.26 - V) / (e^{(19.26-V)/10} - 1)$$

$$\beta_a(V) = 0.009e^{-V/22.03}$$

$$\alpha_b(V) = 10^{-6}e^{-V/16.26}$$

$$\beta_b(V) = 1 / (e^{(29.79-V)/10} + 1)$$

$$I_{\text{NCa}} = G_{\text{NCa}}(V, t) \cdot (V - E_{\text{Ca}})$$

$$G_{\text{NCa}}(V, t) = g_{\text{NCa}}^{\text{max}} \cdot c^2(V, t) \cdot d(V, t)$$

$$\alpha_c(V) = 0.19(19.88 - V) / (e^{(19.98-V)/10} - 1)$$

$$\beta_c(V) = 0.046e^{-V/20.73}$$

$$\alpha_d(V) = 1.6 \cdot 10^{-4}e^{-V/48.4}$$

$$\beta_d(V) = 1 / (e^{(39-V)/10} + 1)$$

$$I_{\text{LCa}} = G_{\text{LCa}}(V, t) \cdot (V - E_{\text{Ca}})$$

$$G_{\text{LCa}}(V, t) = g_{\text{LCa}}^{\text{max}} \cdot e^2(V, t)$$

$$\alpha_e(V) = 15.69(81.5 - V) / (e^{(81.5-V)/10} - 1)$$

$$\beta_e(V) = 0.29e^{-V/10.86}$$

Calcium-Dependent Potassium Currents. Experimental data indicate that BK and SK calcium-activated potassium channels are present in rat hippocampal dentate granule cells (Beck et al., 1997). BK channels have a high unitary conductance (≥ 100 pS) and are highly voltage- and calcium-sensitive, while SK channels have a lower single-channel conductance (5 to 20 pS), are poorly voltage sensitive or voltage insensitive, but are highly calcium-sensitive (Latorre et al., 1989; Sah, 1996). The macroscopic currents corresponding to the activation of these channels have been identified and named as I_C and I_{AHP} , respectively. Functionally, the activation of I_C contributes to final spike repolarization, fast hyperpolarization, and early adaptation, while I_{AHP} contributes to the slow-phase of hyperpolarization following action potentials and is largely responsible for the spike-frequency adaptation observed in the hippocampal granule cells exposed to prolonged depolarizing current pulses (Beck et al., 1997; Lancaster et al., 1991). I_C can be blocked by TEA or CTX, while SK channels are relatively insensitive to TEA but sensitive to apamine (Beck et al., 1997).

The equations for the BK calcium activated potassium current were taken from De Schutter and Bower (1994):

$$\begin{aligned} I_C &= G_{BK}(V, [Ca^{2+}], t) \cdot (V - E_K), \\ E_K &= -85 \text{ mV} \\ G_{BK}(V, [Ca^{2+}], t) &= g_{BK}^{\max} \cdot r(V, t) \cdot s^2([Ca^{2+}]) \\ \alpha_r(V) &= 7.5 \\ \beta_r(V) &= 0.11/e^{(V-35)/14.9} \\ s_{\infty} &= 1/(1 + 4/[Ca^{2+}]) \\ \tau_s &= 10. \end{aligned}$$

Although these channel kinetics were derived for Purkinje cells, the main properties are similar to those reported for other neuron types including DG cells (Beck et al., 1997).

The equations for the SK calcium-activated potassium current were taken from Yuen and Durand (1991) with some of the parameter values modified to be more consistent with the data referenced above. The activation curve was shifted 12 mV toward more positive values to match more closely the threshold for activation, and the activation curve slope was reduced. Also the time constant was 1.67 times slower than in Yuen and Durand (1991) to fit better the adaptive properties:

$$\begin{aligned} I_{AHP} &= G_{SK}([Ca^{2+}]) \cdot (V - E_K), \\ E_K &= -85 \text{ mV} \\ G_{SK}([Ca^{2+}]) &= g_{SK}^{\max} \cdot q^2([Ca^{2+}]) \\ \alpha_q([Ca^{2+}]) &= 0.00246/e^{(12 \cdot \log_{10}([Ca^{2+}]) + 28.48)/-4.5} \\ \beta_q([Ca^{2+}]) &= 0.006/e^{(12 \cdot \log_{10}([Ca^{2+}]) + 60.4)/35}, \end{aligned}$$

where the intracellular calcium concentration is given in μM .

Distribution of Ionic Conductances. Although values for channel densities are not well known, recent work suggests that active conductances exist in dendrites as well as in the soma and axon.

To estimate parameter values for sodium and delayed rectifier potassium currents, the firing threshold and amplitude of APs at different sites in DG cells were considered. Jefferys (1979) and more recently Foster and Richardson (1997) have shown that sodium dependent APs travel 100 to 250 μm up granule cell

dendrites at a velocity of 80 to 120 $\mu\text{m}/\text{ms}$ whether they are synaptically induced or induced by antidromic stimulation. Several parameter sets were found to be consistent with these data.

Though kinetic analysis and pharmacological properties are available for A-type potassium channels, very little is known about their distribution in DG cells. In our model A-type channels were distributed to delay effectively the onset of APs.

A number of studies at both the macroscopic level and the single-channel level have described multiple components of calcium currents at different sites in DG cells (Blaxter et al., 1989; Fisher et al., 1990; Eliot and Johnston, 1994). Single-channel studies give estimates of the relative distribution of T-, N-, and L-type channels in the DG cell somata, while whole cell recordings suggest that the different channel types are differentially distributed in the dendrites (Blaxter et al., 1989; Eliot and Johnston, 1994). A greater proportion of L-like current was found in the somatic and perisomatic region by Blaxter et al. (1989), and Ahljianian et al. (1990) found L-type channels to be located primarily in the base of proximal dendrites. The N-like channels are enriched in dendrites, especially in distal parts of dendrites (Blaxter et al., 1989). However, this N-like current may have included both N and P-type calcium currents (Eliot and Johnston, 1994). A T-like current could be elicited from all parts of the neuron (Blaxter et al., 1989; Zhang et al., 1993), although T channels may have larger densities in dendrites (Zhang et al., 1993; Eliot and Johnston, 1994; Fisher et al., 1990). The experimental data for calcium channel distributions summarized in Table 2 led us to choose parameter values given in Table 3.

The distribution of calcium activated potassium channels is not known, although there is some experimental evidence (Roberts et al., 1990; Robitaille et al., 1993) suggesting that calcium channels and calcium activated potassium channels are colocalized. The possible colocalization of the calcium-related channels imposed some constraints on the model and simulations were done to suggest likely pairings and distributions in different regions of the cell.

Results

To construct a proper model of a hippocampal DG cell, we first created a reduced model (1) to explore the underlying ionic mechanisms of the DAP and the AHP, (2) to investigate the possible coactivation of

Table 2. The relative distributions of Ca²⁺ channels in hippocampal DG cells.

	T-type	N-type	L-type
Soma	Low ~10%	High ~100%	Low ~5%
	(Fisher et al., 1990)	(Fisher et al., 1990)	(Fisher et al., 1990)
	Exist	Low	High
	(Blaxter et al., 1989)	(Blaxter et al., 1989)	(Blaxter et al., 1989)
	~20%	N and P ~40%	~40%
	(Eliot and Johnston, 1994)	(Eliot and Johnston, 1994)	(Eliot and Johnston, 1994)
PD	Exist	High	High
	(Blaxter et al., 1989)	(Blaxter et al., 1989)	(Blaxter et al., 1989; Ahlijanian et al., 1990)
	~20%	N and P ~40%	~40%
	(Eliot and Johnston, 1994)	(Eliot and Johnston, 1994)	(Eliot and Johnston, 1994)
MD	Exist	High	Low
	(Blaxter et al., 1989)	(Blaxter et al., 1989)	(Blaxter et al., 1989)
DD	Exist	High	Low
	(Blaxter et al., 1989)	(Blaxter et al., 1989)	(Blaxter et al., 1989)
	High		
	(Zhang et al., 1993)		

Note: The different estimates are based on either somatic patch clamping or on whole cell recordings from slices or dissociated neurones. PD, proximal dendrites; MD, middle dendrites; DD, distal dendrites.

 Table 3. Channel densities (mS/cm²) of the model DG cells.

	Axon	Soma	GCLD	PD	MD	DD
Na	210	120	18	13	8	0
fK _{DR}	28	16	4	4	1	1
sK _{DR}	0	3	3	3	3	4
K _A	4	12	0	0	0	0
T	0	0.15	0.3	1	2	2
N	0	2	3	1	1	1
L	0	10	15	15	1	0
BK	0	0.3	0.3	0.5	1.2	1.2
SK	0	0.5	0.2	0.1	0	0

Note: These parameters correspond to the model control case. When channel blockers were applied, the experimental data were reproduced by reducing the densities of the affected channel types.

different types of calcium and calcium-dependent currents according to their colocalization, and (3) to give a first approximation of the distribution of active channels necessary to reproduce characteristic firing patterns of DG cells. These channel densities from the reduced model were modified in more detailed models, to account for the different morphologies and

to reproduce physiological measurements either under normal physiological conditions or when blocking agents were applied. The model was then used to explore possible reasons for the resistance of DG cells to epileptogenic bursting behavior.

Effects of Delayed Rectifier Currents on the DAP

To assess the effects of delayed rectifier currents on the DAP, we used reduced models composed of either a soma and axon alone or a soma, axon, and dendrites. Parameter values for sodium and potassium conductance densities were chosen to reproduce the amplitude and width of action potentials typically observed in DG cells. No calcium channels were included in this set of simulations.

We found that a large DAP could be produced by capacitive discharge of the dendrites but that this DAP could be suppressed by dendritic sK_{DR} currents (Fig. 2). When the reduced model contained only a soma and axon with sodium and fK_{DR} conductances, the response to brief current injection at the soma was a single action potential with no DAP. However, when two dendritic trees containing sodium and fK_{DR} channels were

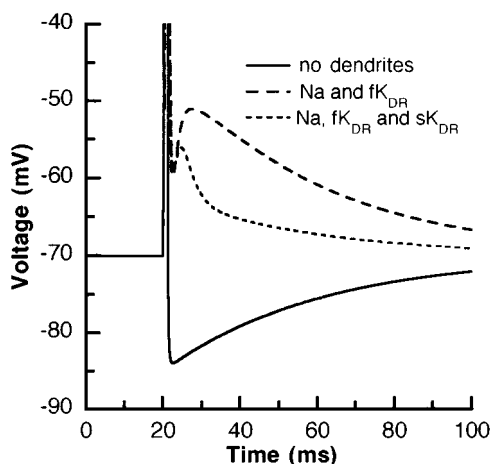


Figure 2. Effects of delayed rectifier currents on the generation of the DAP. A model without dendrites did not produce DAP-like membrane voltage changes when Na^+ and fK_{DR} channels were present. When dendrites were attached to the soma, a DAP was generated due to capacitive discharge of the dendrites when the dendrites contained the same two channel types although with lower densities. This DAP could be suppressed by replacing some of the fK_{DR} channels in the dendrites by sK_{DR} channels in the dendrites. The current stimulus was 2 nA lasting 0.5 ms.

attached to the soma, the same stimulus evoked an AP followed by a large DAP generated by the capacitive discharge of the dendritic tree. This DAP was substantially reduced when sK_{DR} channels were included in the dendrites. The results in Fig. 2 are shown for the case when half of the dendritic fK_{DR} channels were replaced by sK_{DR} channels.

The reduced model results suggested specific distributions for fK_{DR} and sK_{DR} channels. The K_{DR} channels at the soma and in the axon had to be predominantly fast K_{DR} for the simulated AP to have the proper width. Dendritic K_{DR} channels had to be a mix of fast and slow K_{DR} channels to suppress the DAP. This was necessary, as discussed further below, because experimental results suggest that calcium currents are responsible for the DAP in DG cells.

Effects of Calcium Currents on the DAP

Simulations were done with the reduced model to address the question of which calcium channel types could contribute to the emergence of the DAP. The different calcium channels were included in the model separately, and the possible role of their location was also assessed. The distributions of sodium and delayed rectifier potassium channels were chosen as in Table 3,

and calcium channels were included in either the soma or the dendrites.

T, N, L Channels at the Soma. When T, N, or L channels were included at the soma, only the activation of T-type calcium channels could contribute significantly to the generation of the DAP (Fig. 3A). Although the L and N channels had only a small effect on DAP amplitude compared to the control case with no

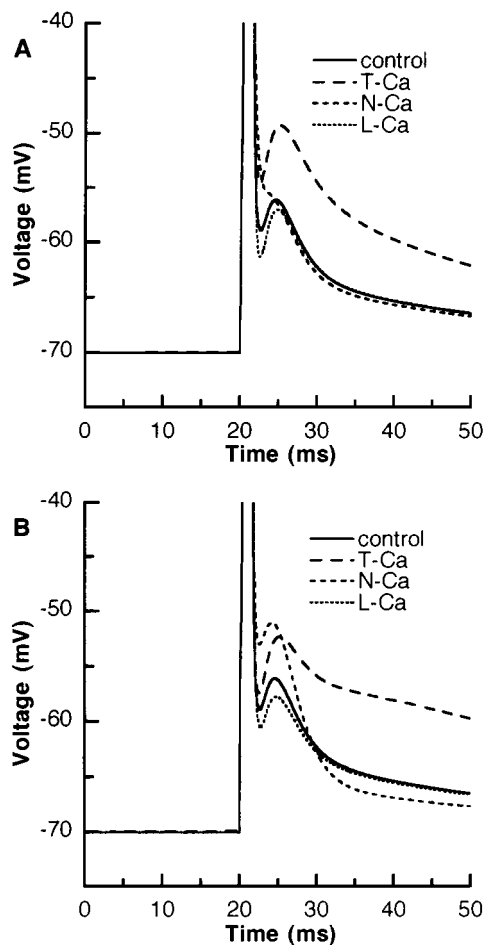


Figure 3. Contribution of somatically or dendritically distributed T, N, or L channels to the generation of the DAP. A: A model with sodium and delayed rectifier currents in which the DAP was largely suppressed was considered as the control case. Simulation results are shown when 1,000 T, N, or L calcium channels were in the soma membrane. Only T channels could contribute significantly to the generation of the DAP. Activation of N channels caused spike broadening, and L channels had little effect. B: When 200 T, 500 N, or 500 L channels were included in the dendrites, T channels but also N channels could enhance the DAP while L channels still had no significant effect.

calcium channels, they did have other effects. N channels caused a slight spike broadening and eliminated the postspike dip before the DAP, while L channels enhanced the fast-spike repolarization. This latter effect can be explained by the fact that the additional depolarization due to L channel activation enhanced activation of the potassium channels, in particular sK_{DR} ; however, the L channel current was very brief and was not present to oppose the enhanced potassium currents during the afterpotentials.

T, N, L Channels in the Dendrites. When a T, N, or L channel was included in the dendrites, both T and N channels could contribute significantly to the generation of the DAP (Fig. 3B). However, with N channels, the DAP amplitude was smaller and the width was narrower compared to that with T channels. The effect of dendritically distributed L channels on the DAP was similar to that when L channels were included in the soma: spike repolarization was enhanced, and DAP amplitude was reduced compared to the control case with no calcium channels. We note that the density of T channels in the dendrites had to be small. If not, the DAP became much prolonged, and burst discharges occurred.

Cooperative Behavior of Calcium-Related Channels

Calcium influx is known to activate fast and slow calcium-dependent potassium channels, which control the early and late phases of DG cell after-hyperpolarization, respectively. Simulations were done with the reduced model to determine possible combinations of specific calcium and calcium-dependent potassium channel types that would produce an appropriate AHP in response to brief current injection. Results were compared to those obtained earlier when calcium channels but not calcium-dependent potassium channels were included in the soma.

BK with T, N, or L Channels. When BK channels were paired with T, N, or L type calcium channels, T channels were found to be more effective in activating BK channels than N or L channels (Fig. 4A). In fact N and L channels paired with BK channels had only a small effect compared to the control case with no BK channels (Fig. 4B, C). In the simulations there were 1,000 calcium channels (T, N, or L) and 100 BK channels at the soma. Given typical values for single channel

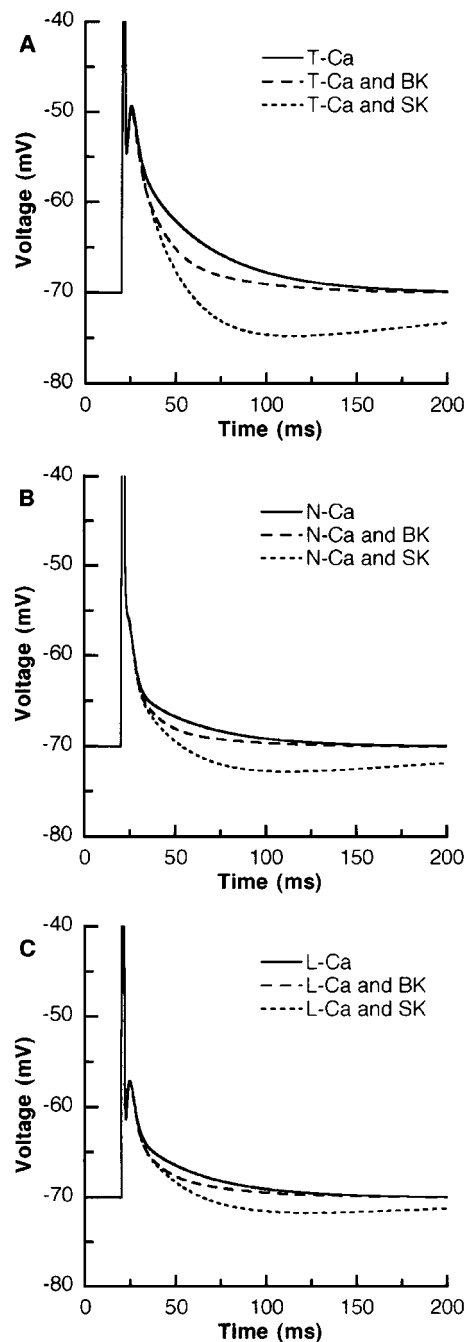


Figure 4. Coactivation of different types of calcium and calcium dependent potassium channels. The parameters for sodium and delayed rectifier potassium currents were those in Table 3. A: 1,000 T (solid line), 1,000 T and 100 BK (dashed line) or 500 SK (dotted line). B: 1,000 N (solid line), 1,000 N and 100 BK (dashed line) or 500 SK (dotted line). C: 1,000 L (solid line), 1,000 L and 100 BK (dashed line) or 500 SK (dotted line) channels were included in the soma.

conductances this means that maximum conductances were 1.8, 3.16, 5.64, and 2.26 mS/cm² for T, N, L, and BK channels, respectively. The T channel was the most effective despite having the lowest maximum conductance because of its lower threshold for activation.

SK with T, N, or L Channels. When SK channels were paired with T, N, or L calcium channels, large hyperpolarizations were obtained in all cases but particularly with the T channel pairing (compare Fig. 4A with 4B and 4C) (again because T channels have a lower threshold for opening, allowing more calcium to enter at lower voltage changes). While the effect of coactivation of BK and T channels was much stronger earlier than later, activation of SK and T channels caused a prolonged large AHP. N and L channels still could significantly activate SK channels, but the resulting AHP was much less than with T channels. Because of the low single-channel conductance of an SK channel, 500 SK channels were included the soma in these simulations corresponding to a maximum conductance of 1.35 mS/cm². The high sensitivity of SK channels to calcium concentration changes is what made the pairing with N and L channels much more effective than the pairing of BK channels with N and L channels.

Responses to Current Injections under Normal Conditions

Using the insights gained with the reduced model together with experimental data, conductance densities were chosen for the full morphology DG cell model (Fig. 1). Responses to current injections with different amplitudes and durations were compared to published data (Zhang et al., 1993; Spruston and Johnston, 1992; Staley et al., 1992). Several sets of conductance densities were found that could produce results similar to the published recordings. However, constraints imposed by data from experiments with channel blockers, as noted below, limited the ranges of possible conductance density values.

Final parameter value choices for the full morphology DG cell model were those given earlier in Table 3. Comparisons of simulated data using these final parameter value choices with published data are given below.

The simulated response to a short but very strong stimulus applied at the soma reproduced qualitatively that obtained by Zhang et al. (1993) as shown in

Fig. 5A. We paid special attention to reproduce the amplitude (about 90 mV measured from the threshold) and the width ($V_{1/2} = 2$ ms) of the AP at the soma and the back-propagation velocity and attenuation of the AP measured at different dendritic sites as suggested by data from Jefferys (1979). The threshold for firing was between -55 and -48 mV as suggested by the experimental data. The spatial distribution and densities of different calcium-related channels were chosen to fit the broad and large DAP.

The simulated responses of the DG cell to a less strong, but longer depolarizing current injection reproduced the recordings of Spruston and Johnston (1992) as shown in Fig. 5B. A family of voltage traces with respect to both sub- and suprathreshold phenomena is shown. The input resistance of our model neuron was half the input resistance of the particular DG cell studied by Spruston and Johnston (1992), so simulated and experimental results should be compared when input currents are twofold stronger in the simulations than in the experiments. When the amplitude of the current injection was 60 pA in the simulation, two action potentials were generated during the 500 ms stimulus period. The delay of the onset of firing (100 to 150 ms) and the interspike interval (more than 200 ms) match the Spruston and Johnston (1992) data qualitatively. Our model and the recorded DG cells showed only subthreshold phenomena when the amplitude of the current injection was smaller. The responses of the DG cell to hyperpolarizing currents with different amplitude were reproduced qualitatively as well.

Figure 5C shows the case when the current injection was 55 pA in the simulated cell and 50 pA in an experiment with a neuron having a lower resting potential (Spruston and Johnston, 1992). In these cases only a single AP could be evoked during the current stimulus period, and instead of the second spike only a large depolarization appeared.

The simulated response of the DG cell to a long-lasting stimulus reproduced that given by Staley et al. (1992) with characteristic early and late adaptive behavior (Fig. 5D). In both the simulated and the measured traces 9 to 12 APs were evoked during the 500 ms current stimulus, each AP (except for the first few spikes) was followed by a DAP, and the interspike intervals showed a gradual increase with time.

The key steps in finding channel densities corresponding to particular characteristics of these experimental data were (1) determining sodium and delayed rectifier potassium channel densities to obtain APs at

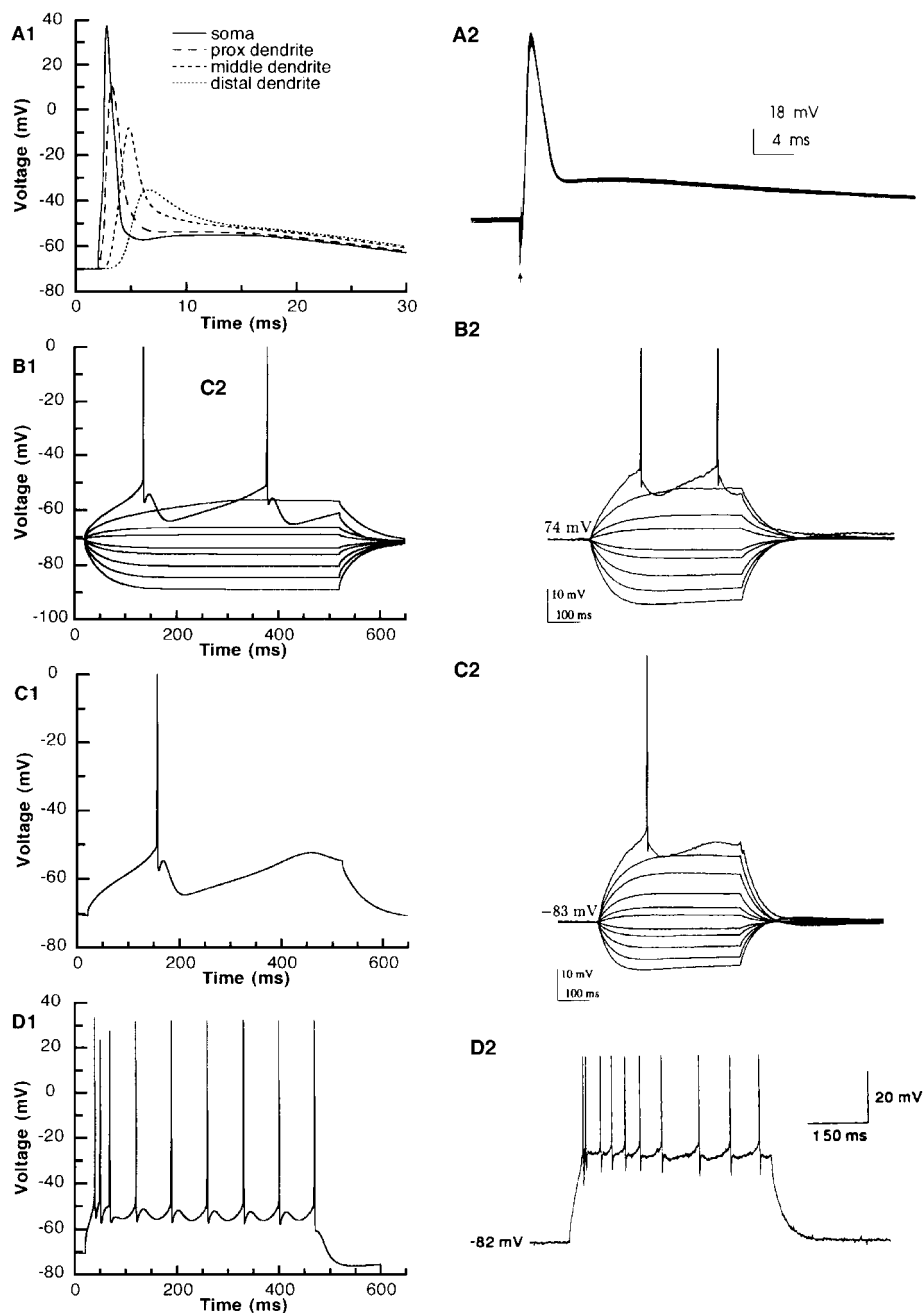


Figure 5. Comparison of simulation results with experimental recordings of responses of DG cells to current injections. A1: The model DG cell's response to a 0.5 ms, 2 nA current injection into the soma. Voltage changes measured at soma, proximal, middle, and distal dendrites are shown. A2: Superimposed APs and DAPs antidromically evoked from granule cells (600 pA, 5 ms) reported by Zhang et al. (1993, Fig. 2A). B1: Simulation of family of voltage responses of the model granule cell (60, 40, 20, 10, -10, -20, -40, -60, -80 pA, 500 ms) to both depolarizing and hyperpolarizing current injections. B2: Experimental traces of action potentials and subthreshold changes in response to current injections with different amplitudes (30, 20, 10, 5, -5, -10, -20, -30, -40 pA, 500 ms) reported by Spruston and Johnston (1992, Fig. 6A1). The difference between the amplitude of modeled and experimental current injections is due to the difference between the model DG cell input resistance and the input resistance of the DG cell from which the recordings were taken. C1: In response to a current injection with amplitude 55 pA (500 ms) a single action potential could be evoked in the simulated cell and only a subthreshold depolarization appeared instead of the second spike. C2: The same observation was made by Spruston and Johnston (1992, Fig. 6A2) for a DG cell with lower resting potential. Adaptive properties D1: simulated with the model and D2: measured by Staley et al. (1992, Fig. 3) in response to a 200 pA, 500 ms current step. Both the early and the later phases of adaptation could be reproduced. Channel densities in the model were the same in all of these simulations. A2, B2, C2, and D2 reproduced with permission of The American Physiological Society.

different sites with the proper amplitudes, (2) introducing an A-type potassium conductance to reproduce the delay of the onset of AP, and (3) matching the width and the amplitude of the DAP and reproducing adaptive properties by including mostly T and BK channels into the more distal dendrites and N, L, and SK channels into the soma and more proximal dendrites.

Generation of Calcium Spikes in the Presence of Channel Blockers

Some responses of DG cells to current injections could be reproduced by choosing parameter values from a relatively wide range. However, simulating experimental recordings when different channel blockers were applied allowed us to reduce these wide ranges of possible values and more precisely test our model DG cell. A number of parameter sets could reproduce experiments with channel blockers, too. The final set of parameter values was chosen from those sets that could reproduce qualitatively both the experiments in normal solution and with channel blockers.

In the following simulations the final chosen parameter set (the values given in Table 3) is referred to as the control case. Although, the effects of channel blockers may be very complex, we modeled their effects by reducing the maximal conductance values for particular channel types known to be sensitive to the applied blocking agent. Simulations with channel blockers assumed that sodium channels were blocked 100% by TTX; fast and slow K_{DR} , BK, SK, and K_A channels were blocked 90% by Ba^{2+} ; fast and slow K_{DR} and BK channels 20 to 90% by TEA; A-type potassium channels 50% by 4 AP; and T-type calcium channels were blocked 50 to 100% by Ni^{2+} or Co^{2+} .

Application of TEA. A series of slow spikes and plateau potentials were elicited by very short depolarizing current pulses when TEA application was simulated (Fig. 6A1). The effect of TEA application as measured by Fricke and Prince (1984) (Fig. 6A2) is shown for comparison. In the simulations the maximum conductances of TEA sensitive channels—namely, fK_{DR} , sK_{DR} , and BK channels—were reduced by 85% at the soma and by the same or a lesser amount in the dendrites (because of restricted diffusion of the blocker in dendrites). The strength and duration of the stimulus in the experiment and in the simulation were similar and in both cases the cell responded with a series of long-lasting plateau potentials.

Application of TEA and TTX. Slow plateau potentials and calcium spikes were measured after application of TEA and TTX. When sodium channels were blocked and 90% of TEA sensitive potassium channels in the soma and GCL dendrites and a gradually decreasing proportion in the more distal parts of the dendrites were also blocked, the simulated results (Fig. 6B1) closely resembled recordings from Blaxter et al. (1989) (Fig. 6B2).

To reproduce the experimentally measured calcium spikes, especially the subthreshold phenomenon recorded by Blaxter et al. (1989), we had to assume that blockage of different TEA sensitive potassium channels was not perfect and that the density of the still unblocked potassium channels in the distal dendrites might be higher than they were in the other regions. This would be consistent with dendritic branching and thinning, making the distal dendrites less reachable by channel blockers.

We found that all three calcium channel types made some contribution to the evoked calcium spike wave form. The onset of the calcium spike and the faster early peak was caused mainly by T and N channels, while the amplitude of the slow spike was due to the sum of all calcium-channel densities. The duration of the calcium spike was determined mostly by the L channel density.

Replacement of Ca^{2+} by Ba^{2+} . Simulation of the substitution of Ba^{2+} for Ca^{2+} in a perfusion solution resulted in the development of slow membrane depolarizations in DG cells similar to that found by Fricke and Prince (1984) (Fig. 6C). The effect of Ba^{2+} is presumably its ability to substitute Ca^{2+} while blocking potassium channels. To model the effects of Ba^{2+} perfusion we reduced the conductances of TEA sensitive potassium channels, as in the previous simulation, and also blocked the SK and A-type channels. To obtain a close fit to the experimental data, the maximal conductances of these potassium channels were set to 10 or 50% of their original values, respectively. Thus a longer slow spike could be evoked by a very short current stimulus in agreement with the experiments.

Replacement of Ca^{2+} by Ba^{2+} and Application of TTX. When in addition to Ba^{2+} perfusion TTX was also applied, the early fast component of the calcium spike was eliminated both in the experiment (Fig. 6D2) and in our simulation (Fig. 6D1). The model also

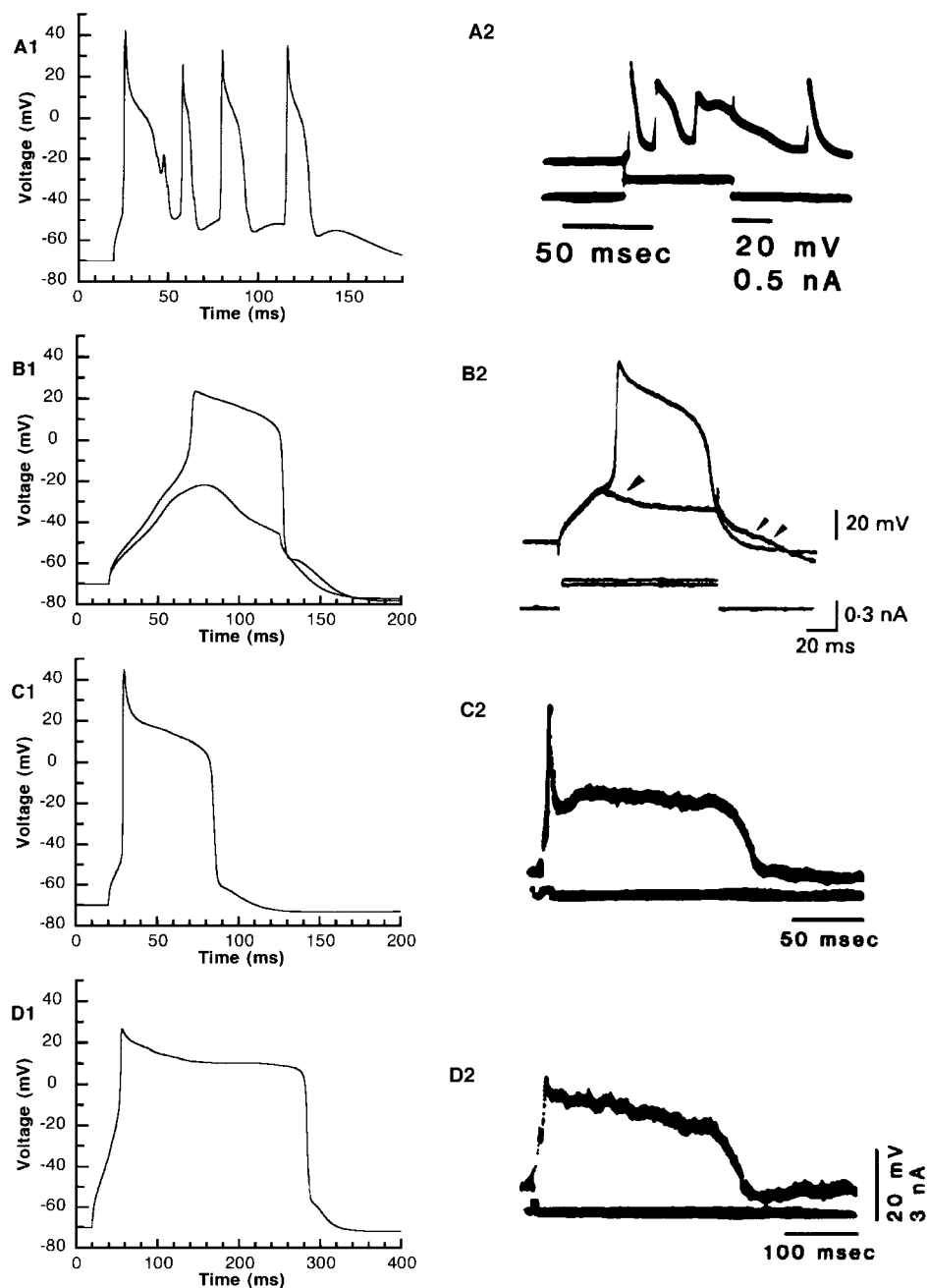


Figure 6. Simulation of the effects of different channel blockers. A1: Simulation of application of TEA. fK_{DR} , sK_{DR} , and BK channels were blocked by 80 to 85%. Current step was 400 pA for 30 ms. A2: Typical response of DG cell to depolarizing current step in 5 mM TEA (Fricke and Prince, 1984, Fig. 8B). B1: Simulation of calcium spikes in dentate granule cells. Sodium channels were eliminated, and TEA sensitive channels at the soma were reduced by 90% of their original values. Injected current was 200 pA for subthreshold changes and 240 pA to initiate calcium spike. Stimulus duration was 100 ms. B2: Similar broad spikes could be evoked by depolarizing current injection when 1 μ M TTX and 10 mM TEA were applied (Blaxter et al., 1989, Fig. 1B). Both the simulated and the measured calcium spikes were followed by an AHP thought to be caused by an SK-type Ca^{2+} -dependent potassium current that was not affected by low TEA concentrations. C1: Simulation of responses of DG cells in Ba^{2+} perfusion. TEA-sensitive potassium channels were reduced as in the previous simulation. A-type and SK channels were reduced by 50 or 90%, respectively. Brief current injection (300 pA, 10 ms) was applied at the soma. C2: The effect of replacing Ca^{2+} by Ba^{2+} as measured by Fricke and Prince (1984, Fig. 9B1). D1: Simulation of the effect of replacing Ca^{2+} by Ba^{2+} and application of TTX. The early fast component in response to a current stimulus (300 pA, 35 ms) was eliminated by TTX application. In addition to the changes made in case C, sodium channels were totally reduced. D2: DG cell response after Ba^{2+} perfusion and application of TTX measured by Fricke and Prince (1984, Fig. 9B2). A2, C2, and D2 reproduced with permission of The American Physiological Society. B2 reproduced with permission of The Physiological Society (London).

showed that the slow spike was resistant to TTX, and the duration of the plateau potential was prolonged when TTX was applied. The increase of plateau duration was at least twofold in both the experiment and the simulation.

Effect of Channel Blockers on the DAP

Almost all of the effects of channel blockers on the generation of the DAP investigated by Zhang et al. (1993) could be closely reproduced by our model (Fig. 7). When Zhang et al. (1993) applied TTX, short depolarizing currents could still evoke DAPs (Fig. 7A2). When sodium channels were completely blocked in the simulation, similar responses (Fig. 7A1) were found. In the simulations short-duration stimuli did not evoke DAPs, while longer duration stimuli did evoke DAPs with different amplitudes. The results agree with Zhang et al. (1993) qualitatively in showing that TTX sensitive sodium conductances are not necessary for DAP generation.

In simulations and experiments, the presence of TEA and 4-AP enhanced the DAP and prolonged the APs evoked by the same short stimulus (Fig. 7B). Twelve minutes after the application of TEA and 4-AP, a calcium spike was recorded from the DG cell (Zhang et al., 1993). Our simulation results are shown when potassium channels except SK channels were reduced by 20, 40, 80, or 90% compared to their original values (to simulate different times after blocker application). The results demonstrate the robustness of the DG cell (and the DG cell model) in some respects. When there was a 10 to 15% reduction in the maximum conductances of TEA sensitive channels, the characteristic features of the DG cell response were preserved. When the potassium channels were reduced by 20%, a larger and broader DAP appeared. When the reduction was 40%, a double spike could appear, and for an 80% reduction the APs in this double spike became wider. For 90% reduction of potassium channels, a calcium spike could be evoked from the model DG cell.

Several chemicals, including Ni^{2+} and Co^{2+} , have been reported to block low-threshold T-type calcium channels (Fig. 7C2) and thus to abolish the DAP. Our simulations produced the same phenomena when the maximal conductance for T channels was reduced (Fig. 7C1). Results are shown when the T channel conductance was reduced 50 or 100% (completely blocked).

Channel Types Involved in the Resistance of DG Cells to Epileptogenic Burst Discharges

Although some suggestions have been made to explain why DG cells are usually resistant to bursting behavior (Köhr and Mody, 1991; Beck et al., 1997), the underlying mechanisms of this resistance are not clear. We used our model to indicate which channel types and densities might confer this resistance on DG cells and to explore changes in channel densities that might lead to bursting behavior. Although the model showed burst-like firing when T channel densities were increased, this bursty behavior could be converted to physiological spiking by increasing the potassium channel densities (simulation results are not shown). However, the DG cell model already contained densities of calcium channels (and in particular T channels) comparable to those in hippocampal pyramidal cell models with bursting (Migliore et al., 1995), suggesting that the difference between the spiking behavior of these cell types cannot be explained in terms of calcium channel densities. It might be more plausible to express the conversion of a DG cell from physiological to pathological behavior in terms of loss or block of some of the voltage-activated potassium channels. Among the potassium channels, BK, SK, and especially sK_{DR} channels were found to have a large inhibitory effect on the excitability of the model DG cell, but fK_{DR} or K_{A} channels did not. When the density of sK_{DR} channels in dendrites was selectively reduced by 90%, the model DG cell produced a long-lasting fast burst of spikes in response to a very short but strong current injection (Fig. 8A). When sK_{DR} channels were replaced by fK_{DR} channels, a similar fast burst appeared. Elimination of BK and SK channels along the cell led to a slower burst-like firing in response to the same stimulus (Fig. 8B). The results suggest that potassium channels, and in particular the sK_{DR} channels, may play an important role in preventing epileptogenic burst discharges in DG cells.

Modulatory Effect of Changes in Buffering Capacity

Reduced calcium buffering capacity has been seen following epileptogenesis (Beck et al., 1997; Vreugdenhil and Wadman, 1995). The effect of changes in buffering capacity was studied in the model DG cell by altering the calcium removal rate (Fig. 9). This is a simplification because the removal rate includes removal by diffusion, pumps, and buffers. Furthermore, this does not consider return of calcium by release from buffers,

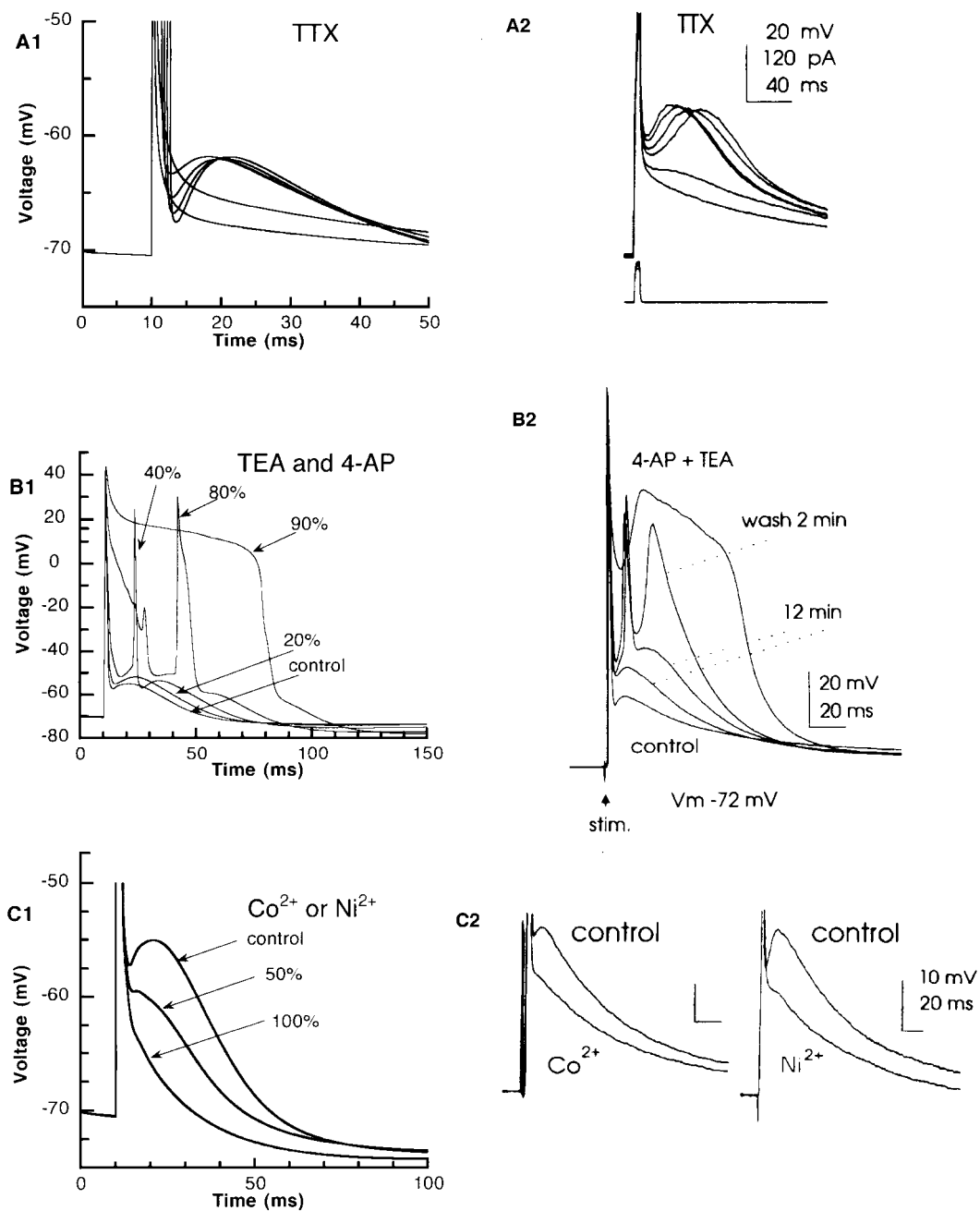


Figure 7. Simulation of the effects of bath application of different chemicals on DAP generation. The parameter values for the control case are given in Table 3. A1: To simulate the effect of application of TTX, the sodium conductances were eliminated. Cases when current injections with different durations (13 nA; 0.05, 0.1, 1, 1.5, 2, 2.5 ms) were applied are shown. A2: Experimental recordings reported by Zhang et al. (1993, Fig. 4D) show the generation of DAPs with graded amplitudes when current injections with different intensities were applied in the presence of 0.5 μM TTX. The slower time course and larger amplitude of the experimental recording can be attributed to a lower temperature. B1: Simulation of the effects of TEA and 4-AP application. Results are shown for cases when conductances of all potassium channel types except SK channels were reduced by 20, 40, 80, or 90%. Current injection was 300 pA, 10 ms. B2: The effects of 2 mM 4-AP and 5 mM TEA reported by Zhang et al. (1993, Fig. 4E) show similar characteristics. C1: Simulation of bath application of Co^{2+} or Ni^{2+} . DAP was partially depressed or totally eliminated when the conductance values for T channels were reduced by 50 or 100%. Current injection was 300 pA, 10 ms. C2: Experiments reported by Zhang et al. (1993, Fig. 8A) demonstrate the effects of 2 mM Co^{2+} and 100 μM Ni^{2+} . A2, B2, and C2 reproduced with permission of The American Physiological Society.

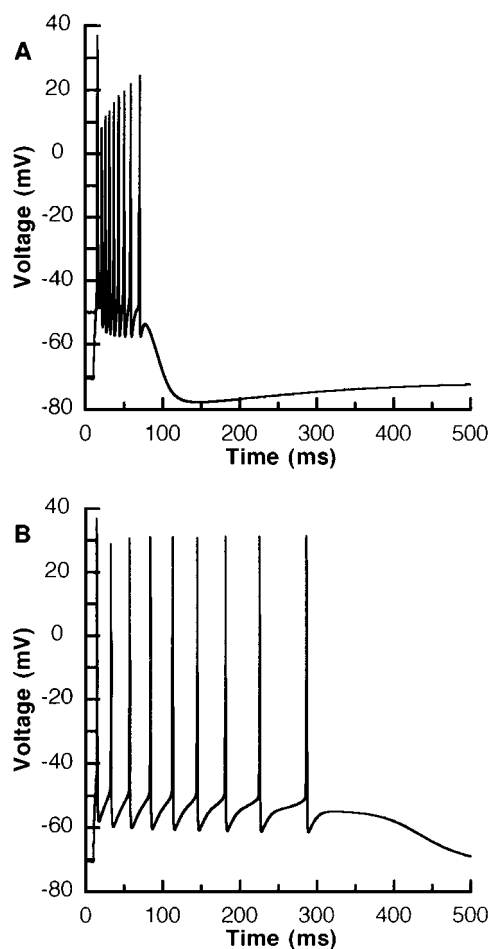


Figure 8. Conditions that might be necessary to render DG cells more bursty. A: Reducing sK_{DR} channel densities by 90% in the dendrites lead to bursting behavior of the model DG cell. B: Eliminating BK and SK channels along the model cell resulted in a slower burst of firing. Previously this stimulus produced only a single spike as shown by the control case in Fig. 9.

which could affect the calcium transient time course. Nevertheless, this simplification provides qualitatively correct changes in calcium transient amplitude. When the calcium removal rate was slower than in the control case, the amplitude of the AHP became larger because of the enhanced effect of calcium-activated potassium channels. When the calcium removal rate was faster than in the control case, the same short but strong current injection evoked sustained repetitive firing. The increased excitability of the model DG cell was due to reduced activation of calcium dependent potassium channels. The results suggest that the reduced calcium buffering capacity observed following epileptogenesis may be a compensatory mechanism to

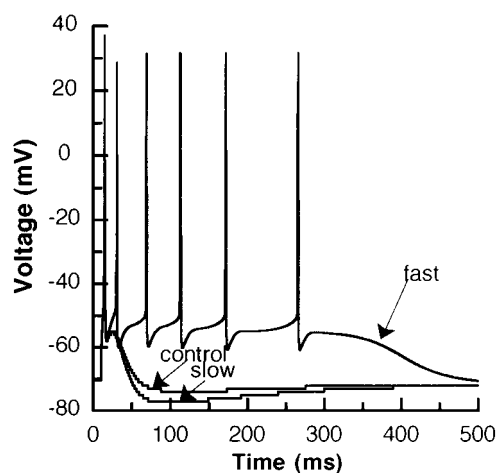


Figure 9. Simulation results with different values of the calcium removal time constant. When the calcium removal rate was faster ($\tau = 1.6$ ms) than in the control case ($\tau = 9$ ms), slow-burst firing was observed similar to that in Fig. 8B. With slower calcium removal rate ($\tau = 18$ ms) the AHP became significantly larger.

reduce excitability by increasing activation of calcium dependent potassium conductances.

Discussion

In this study we constructed a model of a DG cell that would reproduce qualitatively the characteristic responses of DG cells to current injections obtained by different laboratories, including the responses following the application of different channel blockers. The experimental constraints used to construct this model led to important insights regarding the clustering of calcium-related channels, the contributions of the different channel types to the spiking behavior of DG cells, and to the underlying ionic mechanisms of postspike events. We then used the model to suggest explanations for the resistance of DG cells to epileptogenic bursting behavior and to explore the consequences of the reduced buffering capacity observed following epileptogenesis.

Reconstructing Channel Densities from Models and Experimental Data

The spatial distributions and densities of different types of channels in different parts of dentate granule cells are largely unknown. Patch clamp data has been very helpful in determining the existence of a particular

channel type at a particular location (Fisher et al., 1990; Blaxter et al., 1989), but such data have limitations as evidenced by the differing reports summarized earlier in Table 2. Modeling in which results are fit to a large variety of experimental data including data from channel-blocking experiments is another tool that can be used to estimate spatial distributions and densities of channel types. After selecting the channel kinetics for nine different channel types, only the maximal values of channel densities in six functionally different regions of DG cells were considered as free parameters. This still relatively high-dimensional parameter space could be reduced by assuming the possible colocalization of calcium-related channels as supported by both experimental findings (Roberts et al., 1990; Robitaille et al., 1993) and our studies with reduced models. The procedure of reproducing large numbers of experimental recordings and in particular experimental results obtained in the presence of channel blockers, highly constrained the possible values of the remaining free parameters. We do not pretend to have included every conductance present in DG cells or to have determined the precise kinetics or density distributions of the conductances we have included. Nevertheless, the model was highly constrained by experimental data and provided insights into how various conductances may interact.

Densities of sodium and of fast and slow delayed rectifier potassium channels were estimated (1) to fit the threshold of spiking and the amplitude and width of the AP, (2) to suppress the DAP-like event evoked by discharge of the dendritic capacitance, and (3) to reproduce the experimental findings (Jefferys, 1979; Foster and Richardson, 1997) regarding back-propagation of APs into dendrites with proper amplitude and velocity. Consequently, sodium channel density decreased with distance from the soma. The delayed rectifier channels in the soma were primarily of the fast type, while both fast and slow types were present in the dendrites.

Experimental results summarized in Table 2 were used in conjunction with model results to suggest calcium channel distributions. The results suggest that T channels should be located mainly in the middle and distal parts of the dendritic tree, N channels could be located throughout the cell, and L channels should be in more proximal dendrites and the soma. The model with these channel distributions could reproduce the experimentally observed amplitude and duration of the DAP and calcium spikes when different channel blockers were applied.

The densities of calcium dependent potassium channels were chosen to simulate the adaptive properties of DG cells. In response to a long-lasting current injection, the early phase of the adaptation and the large DAPs generated by dendritically distributed T-type calcium channels are controlled by BK-type channels, while the later phase of adaptation is determined by the coactivation and interaction of N- and of L-type calcium and AHP currents. Densities were chosen to allow the model to reproduce (1) the total number of spikes within a certain period of time, (2) the trend in spike amplitude changes within a spike train, (3) the voltage profiles of interspike intervals, and (4) the presence of the DAP and after-hyperpolarization following each spike.

To match the slow onset of firing that can reach 150 ms, we included K_A channels into the model granule cell. Most of the A-type channels were assumed to be in the soma, though some were also included into the axon to cause a further delay in the initiation of the AP. However, a recent paper of Hoffman et al. (1997) studied the A-type potassium channel regulation of signal propagation in dendrites of hippocampal pyramidal neurons and concluded that A-type channels were present throughout the dendritic tree. Whether A-type potassium channels are similarly distributed and might play a similar role in DG cells is not known presently.

The Role of Calcium Dynamics and Clustered Distribution of Calcium Related Channels

Because both I_C and I_{AHP} currents peak relatively quickly, it is thought that the calcium channel(s) and the corresponding calcium-dependent potassium channels should be located close to each other (Roberts et al., 1990; Robitaille et al., 1993). Although very little is known about the possible colocalization of the calcium related channels, there is some indication that calcium influx via N-type calcium channels activates SK channels preferentially to produce the hyperpolarizing current in several cell types (Sah, 1996).

Because of the different time courses and the voltage and calcium sensitivities of calcium-related channels, it is not clear how these channels should interact when all are present in the granule cells at the same time. The deactivation of I_C requires that the intracellular calcium concentration should rise and fall fairly rapidly with every spike. Conversely, I_{AHP} gradually activates during repetitive firing suggesting that intracellular

calcium concentration builds up with each spike. To resolve this contradiction, two pools of internal calcium with different dynamics were described by Warman et al. (1994) in their hippocampal CA1 pyramidal cell model—namely, a rapidly and a slowly decaying pool for mediating I_C and I_{AHP} , respectively. Here we hypothesized, instead, that the different calcium channels and calcium-dependent potassium channels have different and mostly separate spatial distributions.

The model was able to make predictions regarding likely combinations of calcium and calcium-dependent potassium channels based on calcium dynamics. Regardless of calcium channel type, calcium accumulated quickly following discharge of a single action potential. This activated both BK and SK channels causing faster repolarization and a large early and a smaller longer-lasting AHP. Considering the timing and amplitude of the two distinct phases of the AHP, colocalization of T-type calcium channels with BK channels and colocalization of N-type and L-type calcium channels with SK channels seem more likely than other possible combinations.

We addressed the question whether different regions of the DG cell might contain significantly different densities of calcium-related channel types and, if so, what functional role their clustered colocalization might have. Our studies suggested that BK channels with T channels clustering in more distal dendrites and SK channels with N and L channels clustering in more proximal dendrites are likely combinations consistent with experimental data.

To determine possible distributions of calcium-related channels we also considered the fact that the excitability of the DG cell membrane is due largely to the distribution of sodium channels. In our model the proximal, middle, and distal dendrites included gradiently decreasing densities of sodium and fast and slow delayed rectifier currents. The activation of different calcium channel-types is due to the excitability of the membrane where they are located. Thus it seems reasonable to suppose the presence of T-type calcium channels with their low threshold for activation in more distal dendrites and the location of N- and L-type channels with their high threshold activation being more proximal. For the calcium-dependent potassium channels it might be expected that the more voltage-sensitive type is placed in the dendrites because of the importance of local changes in the membrane voltage there. This would lead us to suppose that BK channels should be located more distally where despite their

moderate sensitivity to calcium concentration T channels can still provide enough calcium to activate them. Conversely, SK channels should be located more proximally because of their high calcium sensitivity and insensitivity to membrane voltage. SK channels are activated during long-lasting stimulation of a neuron when the membrane potential repeatedly reaches relatively highly depolarized values and activates calcium channels with higher threshold.

Underlying Mechanisms of the DAP: Calcium Currents Versus Capacitive Dendritic Discharge

Previous modeling results suggested that the DAP was caused by recharging of soma membrane following capacitive discharge of the dendrites in DG cells (Warman et al., 1994; Yuen and Durand, 1991). We also were able to generate a DAP in our model due to capacitive discharge of the dendrites when both the soma and dendrites contained fast sodium and fast delayed rectifier potassium currents. However, Beck et al. (1992) found evidence for the presence of a slowly activating delayed outward potassium current with properties similar to delayed rectifier currents in DG cells. We found that introducing this sK_{DR} current into the dendrites eliminated the DAP-like phenomenon. This led us to believe that the DAP was not caused by capacitive dendritic discharge.

There is much experimental evidence suggesting that calcium currents are responsible for the DAP (Zhang et al., 1993; Blaxter et al., 1989; Brown and Griffith, 1983; Wong et al., 1979). In particular, the DAP can be blocked by Ni^{2+} or Co^{2+} , which have a selective effect on T channels (Blaxter et al., 1989; Zhang et al., 1993; Eliot and Johnston, 1994). However, it is not known where the T channels involved in DAP generation are located or whether other calcium types are also involved. Consequently, we looked at possible contributions of different calcium channel types and their distribution in the cell on the DAP.

The model, with parameter value choices constrained by data from channel-blocking experiments, allowed us to make predictions about the types of calcium and calcium-related channels in DAP generation. Specifically, the model suggested that T-type calcium channels are likely to be the main contributors to the generation of the DAP, whether they are distributed somatically or dendritically. N-type calcium channels located in dendrites may also play a role in forming the DAP, but L-type calcium channels do not. Coactivation

of calcium and calcium-dependent potassium channel types leads to further shaping of the DAP, and the interaction of these currents is responsible for the spike broadening and enhanced DAP seen with bath application of 4-AP and TEA.

Resistance of DG Cells to Epileptiform Burst Discharges

Fricke and Prince (1984) and Blaxter et al. (1989) observed that after hippocampal slices were exposed to TEA, current pulses could evoke slow spikes from DG cells. These spikes were resistant to TTX and therefore presumably mediated by calcium channels. Spontaneous burst discharges or bursts evoked by depolarizing pulses did not occur under these conditions. Though some of the experiments suggest that the large calcium spikes are due to the presence of high densities of N channels (Blaxter et al., 1989), we found that T, N, and L channels can, but differently, contribute to the emergence of calcium spikes.

Various voltage- and calcium-dependent potassium conductances are thought to play an important role in controlling neuronal excitability, and alterations of these membrane currents may be involved in epileptogenesis. Indeed, blocking inhibitory currents in *in vitro* hippocampal slice preparations or in intact animals can result in seizure-like activity patterns (Rutecki et al., 1990) where hippocampal pyramidal and cortical neurons show bursting behavior, but hippocampal DG cells in most cases do not. An interesting question is how can DG cells resist producing such bursting activity despite possessing a relatively large number of calcium channels.

Although the lack of recurrent excitation in the dentate compared to other parts of the hippocampus may play a role, the model suggests that an important explanation for the relatively high resistance of DG cells to epileptiform burst discharges resides in their basic membrane properties, as was suggested by Fricke and Prince (1984). However, it cannot be explained by the absence of calcium conductances because several investigations have indicated the existence of at least three types of calcium channels with high densities in the DG cell soma and in the dendrites, and the DG model here included calcium channel densities comparable to those in other bursting models of hippocampal pyramidal neurons (Migliore et al., 1995).

Although calcium-dependent inactivation of voltage-dependent calcium channels should be also

considered as a protective mechanism in DG cells (Köhr and Mody, 1991; Köhr et al., 1991; Nägerl and Mody, 1998), our studies suggest that the multiple calcium-dependent and voltage-dependent potassium channels with proper densities may be efficient in reducing and regulating the excitability of dentate granule cells. A slow delayed rectifier current was found to be characteristic to DG cells (Beck et al., 1997), and its presence in the dendrites showed a strong ability to suppress bursting behavior in the modeling results presented here. The fast bursting that appeared with selective block of this channel type in the model resembles the high-frequency spike burst observed by Fricke and Prince (1984) in the initial stage of Ba^{2+} perfusion. In addition to sK_{DR} channels, calcium-activated potassium channels, but not fK_{DR} or K_A channels, were also found to be effective in suppressing bursting behavior in DG cells. A role for calcium activated potassium channels in suppressing bursts is consistent with the findings of Pan and Stringer (1996, 1997) that bursts in dentate granule cells could be elicited in reduced extracellular calcium.

Intracellular calcium buffering capacity may also play a role in the resistance of DG cells to epileptogenic bursting behavior. Model results suggest that a lower calcium buffer capacity might increase the resistance to bursting behavior by enhancing the AHP produced by calcium-dependent potassium channels, whereas a high buffer capacity could lead to bursting. A decrease in intracellular calcium buffering capacity in DG and CA1 pyramidal cells has been observed following temporal lobe epilepsy and kindling epileptogenesis (Beck et al., 1997; Vreugdenhil and Wadman, 1995). In agreement with the suggestions made in these studies, the model results indicate that this reduced capacity might be interpreted as a protective mechanism against further bursting.

Acknowledgments

This work was supported by National Institute of Mental Health Grant MH-51081 to W.R. Holmes. We thank W.B. Levy and N.L. Desmond for the anatomical data of the dentate granule cell used in the simulations.

References

- Ahlijanian MK, Westenbroek RE, Catterall WA (1990) Subunit structure and localization of dihydropyridine-sensitive calcium channels in mammalian brain, spinal cord, and retina. *Neuron* 4:819–832.

- Beck H, Clusmann H, Kral T, Schramm J, Heinemann U, Elger CE (1997) Potassium currents in acutely isolated human hippocampal dentate granule cells. *J. Physiol.* 498:73–85.
- Beck H, Ficker E, Heinemann U (1992) Properties of two voltage-activated potassium currents in acutely isolated juvenile rat dentate gyrus granule cells. *J. Neurophysiol.* 68:2086–2099.
- Blaxter TJ, Carlen PL, Niesen C (1989) Pharmacological and anatomical separation of calcium currents in rat dentate granule neurones in vitro. *J. Physiol.* 412:93–112.
- Bower JM, Beeman D (1995) The Book of GENESIS. TELOS, The Electronic Library of Science, Springer-Verlag, Santa Clara, CA.
- Brown DA, Griffith WH (1983) Persistent slow inward calcium current in voltage-clamped hippocampal neurones of the guinea-pig. *J. Physiol. Lond.* 337:303–320.
- Crunelli V, Assaf SY, Kelly JS (1983) Intracellular recordings from granule cells of the dentate gyrus in vitro. In: W Scheifert, ed. *Neurobiology of the Hippocampus*. Academic, New York. pp. 197–214.
- De Schutter E, Bower JM (1994) An active membrane model of the cerebellar Purkinje cell I. Simulation of current clamps in slice. *J. Neurophysiol.* 71:375–400.
- Desmond NL, Levy WB (1982) A quantitative anatomical study of the granule cell dendritic fields of the rat dentate gyrus using a novel probabilistic method. *J. Comp. Neurol.* 212:131–145.
- Desmond NL, Levy WB (1984) Dendritic caliber and the 3/2 power relationship of dentate granule cells. *J. Comp. Neurol.* 227:589–596.
- Desmond NL, Levy WB (1985) Granule cell dendritic spine density in the rat hippocampus varies with spine shape and location. *Neurosci. Lett.* 54:219–224.
- Eliot LS, Johnston D (1994) Multiple components of calcium current in acutely dissociated dentate gyrus granule neurons. *J. Neurophysiol.* 72:762–777.
- Fisher RE, Gray R, Johnston D (1990) Properties and distribution of single voltage-gated calcium channels in adult hippocampal neurons. *J. Neurophysiol.* 64:91–104.
- Foster B, Richardson TL (1997) Current source density analysis of active dendrites in dentate granule cells. *Soc. Neurosci. Abstr.* 27:2007.
- Fox AP, Nowyczyk MC, Tsien RW (1987a) Kinetic and pharmacological properties distinguishing three types of calcium currents in chick sensory neurones. *J. Physiol.* 394:149–172.
- Fox AP, Nowyczyk MC, Tsien RW (1987b) Single-channel recordings of three types of calcium channels in chick sensory neurones. *J. Physiol.* 394:173–200.
- Fricke RA, Prince DA (1984) Electrophysiology of dentate gyrus granule cells. *J. Neurophysiol.* 51:195–209.
- Hines M (1995) Computer modeling methods for neurons. In: MA Arbib, ed. *The Handbook of Brain Theory and Neural Networks*. MIT Press, Cambridge, MA. pp. 226–230.
- Hoffman DA, Magee JC, Colbert CM, Johnston D (1997) K⁺ channel regulation of signal propagation in dendrites of hippocampal pyramidal neurons. *Nature* 387:869–875.
- Jaffe DB, Ross WN, Lisman JE, Lasser-Ross N, Miyakawa H, Johnston D (1994) A model for dendritic Ca²⁺ accumulation in hippocampal pyramidal neurons based on fluorescence imaging measurements. *J. Neurophysiol.* 71:1065–1077.
- Jefferys JGR (1979) Initiation and spread of action potentials in granule cells maintained in vitro slices of guinea-pig hippocampus. *J. Physiol.* 289:375–388.
- Köhr G, Lambert CE, Mody I (1991) Calbindin-D28K (CaBP) levels and calcium currents in acutely dissociated epileptic neurons. *Exp. Brain Res.* 85:543–551.
- Köhr G, Mody I (1991) Endogenous intracellular calcium buffering and the activation/inactivation of HVA calcium currents in rat dentate gyrus granule cells. *J. Gen. Physiol.* 98:941–967.
- Lancaster B, Nicoll RA, Perkel DJ (1991) Calcium activates two types of potassium channels in rat hippocampal neurons in culture. *J. Neurosci.* 11:23–30.
- Latorre R, Oberhauser A, Labarca P, Alvarez O (1989) Varieties of calcium activated potassium channels. *Ann. Rev. Physiol.* 51:385–399.
- Migliore M, Cook EP, Jaffe DB, Turner DA, Johnston D (1995) Computer simulations of morphologically reconstructed CA3 hippocampal neurons. *J. Neurophysiol.* 73:1157–1168.
- Nägerl UV, Mody I (1998) Calcium-dependent inactivation of high-threshold calcium currents in human dentate gyrus granule cells. *J. Physiol.* 509:39–45.
- Numann RE, Wadman WJ, Wong RKS (1987) Outward currents of single hippocampal cells obtained from the adult guinea-pig. *J. Physiol. Lond.* 393:331–353.
- Pan E, Stringer JL (1996) Burst characteristics of dentate gyrus granule cells: Evidence for endogenous and nonsynaptic properties. *J. Neurophysiol.* 75:124–132.
- Pan E, Stringer JL (1997) Role of potassium and calcium in the generation of cellular bursts in the dentate gyrus. *J. Neurophysiol.* 77:2293–2299.
- Rall W, Burke RE, Holmes WR, Jack JJB, Redman SJ, Segev I (1992) Matching dendritic neuron models to experimental data. *Physiol. Rev.* 72, Suppl. 4:159–186.
- Roberts WM, Jacobs RA, Hudspeth AJ (1990) Colocalization of ion channels active zones of hair cells. *J. Neurosci.* 10:3664–3684.
- Robitaille R, Garcia ML, Kaczorowski DJ, Charlton MP (1993) Functional colocalization of calcium and calcium-gated potassium channels in control of transmitter release. *Neuron* 11:645–655.
- Rutecki PA, Lebeda FJ, Johnston D (1990) Epileptiform activity in the hippocampus produced by tetraethylammonium. *J. Neurophysiol.* 64:1077–1088.
- Sah P (1996) Ca²⁺ activated K⁺ currents in neurones: Types, physiological roles and modulation. *Trends Neurosci.* 19:150–154.
- Segal M, Rogawski MA, Barker JLA (1984) A transient potassium conductance regulates the excitability of cultured hippocampal and spinal neurones. *J. Neurosci.* 4:604–609.
- Spruston N, Johnston D (1992) Perforated patch-clamp analysis of the passive membrane properties of three classes of hippocampal neurones. *J. Neurophysiol.* 67:508–529.
- Staley KJ, Otis TS, Mody I (1992) Membrane properties of dentate gyrus granule cells: Comparison of sharp microelectrode and whole-cell recordings. *J. Neurophysiol.* 67:1346–1358.
- Storm JF (1990) Potassium currents in hippocampal pyramidal cells. *Prog. Brain Res.* 83:161–187.
- Vreugdenhil M, Wadman WJ (1995) Potassium currents in isolated CA1 neurons of the rat after kindling epileptogenesis. *Neurosci.* 66:805–813.
- Warman EN, Durand DM, Yuen GLF (1994) Reconstruction of

- hippocampal CA1 pyramidal cell electrophysiology by computer simulation. *J. Neurophysiol.* 71:2033–2045.
- Wong RKS, Prince DA, Basbaum AI (1979) Intradendritic recording from hippocampal neurones. *Proc. Natl. Acad. Sci. USA* 76:986–990.
- Yuen GLF, Durand D (1991) Reconstruction of hippocampal granule cell electro-physiology by computer simulation. *Neuroscience* 41:411–423.
- Zhang L, Valiante TA, Carlen PL (1993) Contribution of the low-threshold T-type calcium current in generating the postspike depolarizing after-potential in dentate granule neurons of immature rats. *J. Neurophysiol.* 70:223–231.